Ab initio study of curvature effects on the physical properties of CH_4-doped nanotubes and nanoropes

2006 J. Phys.: Condens. Matter 18 4649

(http://iopscience.iop.org/0953-8984/18/19/018)

INSTITUTE OF PHYSICS PUBLISHING JOURNAL OF PHYSICS: CONDENSED MATTER

J. Phys.: Condens. Matter **18** (2006) 4649–4675 doi:10.1088/0953-8984/18/19/018

Ab initio study of curvature effects on the physical properties of CH_4-doped nanotubes and nanoropes

B K Agrawal, S Agrawal, S Singh and R Srivastava

Physics Department, Allahabad University, Allahabad 211002, India

E-mail: balkagr@yahoo.co.in and balkagl@rediffmail.com

Received 10 October 2005
Published 27 April 2006
Online at stacks.iop.org/JPhysCM/18/4649

Abstract

We have performed an *ab initio* study of the energetics, structural, electronic, and optical properties of the CH_4-doped ultrathin 4 Å and large diameter carbon nanotubes (CNTs). No adsorption of the CH_4 molecule has been seen either on the groove or on the interstitial sites of the achiral 4 Å nanoropes. In the case of weakly bonded systems such as the adsorption of the CH_4 molecules on the nanotubes, a prominent role of the dispersion forces in the binding is observed. The negative contribution of the zero point vibrational energy to the binding energy is seen to be appreciable. The effects of the tube diameter and the different chiralities of the carbon nanotubes on the adsorbate-induced physical properties have been investigated. In the large diameter tubes, the binding of the CH_4 molecule in the endohedral adsorption is much stronger than that in the exohedral adsorption. The binding of the CH_4 molecules depends upon the chirality of the nanotube and we find no adsorption on the chiral (4, 2) tube. We find that the local density approximation (LDA) over-binds the CH_4 molecule and the generalized gradient approximation (GGA) under-binds it, and for a reliable theoretical estimate one should take some weighted average of the binding energies (BEs) determined in the LDA and the GGA. The currently calculated BE and the adsorbate concentration are in reasonable agreement with the measured data available for the (10, 10) nanotubes. The electronic structure of the pristine tube is quite altered by the adsorption of the CH_4 molecule on the surface of the tube because of the breaking of the symmetry of the host lattice except the chiral (4, 2) tube, which has practically no symmetry. The adsorption incurs splitting in the states in the whole energy range, especially in the large curvature 4 Å tubes. The bandgap of the semiconducting achiral zigzag nanotube is reduced, whereas that of a chiral semiconducting tube is enhanced, by the adsorption of the CH_4 molecules. The adsorption of CH_4 molecules does not alter significantly the peak structure in the optical absorption of the pristine tube, except for some changes in the energy locations and the relative intensities in the achiral tubes. Most of the calculated peaks in the optical absorption of the pristine large diameter (10, 0) and (10, 10) nanotubes have been observed in the experimental measurements.

1. Introduction

There is physisorption of molecules on single-walled carbon nanotubes (SWCNTs) or nanoropes because of their unique structures and reactivity. The physical properties of the SWCNTs such as the electronic, thermal and optical ones etc are affected significantly. One observes very fascinating and important applications like the gas storage (Schlapbach and Zuttel 2001, Hirscher *et al* 2002), electronic and thermal properties (Kong *et al* 2000, Collins *et al* 2000, Sumanasekera *et al* 2000), field emission (Saito *et al* 2002), biotechnology (Shim *et al* 2002), catalysis, differential absorption, nanowire and nanotube production (Tsang *et al* 1994, Ajayan *et al* 1993) etc. The usage of the SWCNTs as templates enables the fabrication of very thin wires and tubes within controllable sizes. One finds practical applications of these products as conducting connects in nanodevices based on molecular electronics. The adsorption may be seen inside the SWCNTs (endohedral) or on the surfaces (exohedral) or at the grooves or the interstitial channels of the bundles of SWCNTs.

Several experiments like the adsorption measurements (Mackie *et al* 1997, Weber *et al* 2000, Talapatra and Migone 2000, Talapatra *et al* 2000) and NMR (Muris *et al* 2000) have been performed on the various inert atoms or molecules like CH_4, C_2H_6, Xe and Ne. The adsorption of the CH_4 molecules on the SWCNTs and the bundles of (10, 10) tubes have been investigated experimentally by several workers (Weber *et al* 2000, Talapatra *et al* 2000, Muris *et al* 2000, Skoulidas *et al* 2002, Kleinhammes *et al* 2003). The values of the Xe coverage and the binding energy have been estimated by them.

Several theoretical calculations at different levels have been performed on the adsorption of the CH_4 molecules (Durgun *et al* 2003, Dresslhaus *et al* 1999, Stan *et al* 2000, Tanaka *et al* 2002, Zhao *et al* 2002, Akai and Saito 2003, Shi and Johnson 2003). In the phenomenological calculations (Stan *et al* 2000, Shi and Johnson 2003), the two-body interactions of Lennard-Jones type were considered for the wide tubes. Shi and Johnson (2003) have performed a grand canonical Monte Carlo simulation using Lennard-Jones potential and have shown that their results for the interstitial adsorption for the heterogeneous SWCNT bundles are in excellent agreement with the experiment for a very low concentration (0.35%) of the CH_4 molecules. A few *ab initio* calculations for the adsorption of CH_4 molecules on the large diameter nanotubes and ropes are available (Tanaka *et al* 2002, Zhao *et al* 2002, Akai and Saito 2003). Tanaka *et al* (2002) have discussed the adsorption on the isolated SWCNT and the idealized slit pore. Zhao *et al* (2002) considered a number of gases adsorbed on SWCNTs and bundles and observed that molecules are adsorbed quite weakly. On the other hand, Akai and Saito (2003) have shown that the binding energy depends considerably on the CH_4 molecular orientation.

All the above *ab initio* calculations are plagued by the following limitations. Firstly, the LDA was used. It is well known that in LDA, an over-binding of the atoms or molecules with the nanotube is seen and one should also investigate the GGA (Dag *et al* 2003). Secondly, the role of the dispersion forces or the vdW interaction was not considered, which is seen to be quite important in the case of weakly bound systems. Thirdly, most of the calculations were performed for the large diameter nanotubes only and no *ab initio* calculation for the adsorption of CH_4 molecules on the small diameter nanotubes and ropes is available. Finally, no contact was made with the experimental measurements. The present investigation fulfils all the above requirements.

The theoretical study of the adsorption of the molecules inside or outside the nanotubes is absolutely essential for understanding the various types of processes and functions such as (i) what the geometries and the types of bonding between the adsorbed molecules and the nanotubes are, (ii) how the physical properties of the nanotubes are affected by the adsorption

of molecules, (iii) how the altered physical properties depend upon the different diameters and chiralities of the nanotubes, etc. In the present study, we address all these questions.

In the present communication, we perform a first-principles study of the adsorption of the CH_4 molecules on the various sites of the small diameter 4 Å SWCNTs and their ropes and also the large diameter nanotubes of different chiralities. The effects of the curvature of the nanotube on the adsorption of CH_4 molecules are also investigated. A fully self-consistent pseudopotential method using the DFT in the GGA as well as in LDA has been adopted. The contributions of the dispersion forces as well as the zero-point vibrational energies have been considered.

2. Method and technical details

We employ the ABINIT code[1], where one uses the pseudopotential and plane waves along with the DFT. The wavefunctions between the real and reciprocal lattices are converted by an efficient fast Fourier transform algorithm (Goedecker 1997). The wavefunctions are determined in a fixed potential according to a state by state or band by band conjugate gradient algorithm (Payne 1992, Gonze 1996). The self-consistent potential is determined by using a potential-based conjugate gradient algorithm. We consider a soft non-local pseudopotential of Troullier and Martins (1991) (TM) within a separable approximation (Kleinman and Bylander 1982) and use the exchange–correlation potential of Perdew *et al* (1996), which is generated by the FHI code (Fuchs and Scheffler 1999). The above method has been successfully applied for the study of the small diameter 4 Å (3, 3) (Agrawal *et al* 2004) and the comparatively large diameter (6, 6) (Agrawal *et al* 2003) nanotubes and their ropes by the present authors.

All the CH_4 molecule–CNT structures have been optimized to achieve minimum energy by relaxing both the lattice constants and the atomic positions in the unit cell, simultaneously. It may be pointed out that the binding energy depends upon the number of chosen k-points in the Brillouin zone (BZ) as well as on the plane wave cut-off energy and one should obtain convergence with respect to both these parameters, a necessary requirement which has been overlooked in earlier publications. The present results have been obtained after achieving convergence w.r.t. to both the number of k-points and the cut-off energy.

In general, the studied structures have been optimized for Hellmann–Feynman forces as small as 10^{-2} eV Å^{-1} on each atom except in some cases where the forces are higher but less than 10^{-1} eV Å^{-1}. Sufficient vacuum space has been chosen to avoid the interference effects between the neighbouring isolated nanotubes in supercell geometries. In all cases, the minimum separation between the CH_4 molecule of one doped tube and the neighbouring doped nanotube was more than 10 Å. The cut-off energy for the plane wave basis was varied from 40 to 90 Ryd for the optimization. For achieving the convergence, a cut-off energy of 80 Ryd for all the nanotubes has been seen to be necessary except the 4 Å (5, 0) nanotube, where a cut-off energy equal to 60 Ryd is found to be sufficient.

The number of atoms in a unit cell of the isolated (3, 3), (5, 0), (4, 2), (10, 0) and (10, 10) nanotubes is 12, 20, 56, 40 and 40, respectively. In the nanoropes, this number of atoms is doubled or tripled for the groove or interstitial sites, respectively.

For establishing the stability of a configuration, we define the chemical binding energy (CBE) of the system by subtracting the optimized energy of the unit cell of the doped nanotube from the sum of the optimized energy of the unit cell of the undoped nanotube and the energy of the isolated chain or chains of the CH_4 molecules adsorbed in or on the doped tube and

[1] The ABINIT code is a common project of the University Catholique de Louvain, Corning Incorporated and other contributors.

divide the difference by the number of the CH_4 molecules in the unit cell. The BE is thus the gain in energy by the adsorption of the CH_4 molecule. A positive value of the CBE favours the adsorption of the CH_4 molecule on or in the nanotube, whereas a negative value of CBE means no CH_4 adsorption. It may be noted that a CH_4 molecule per unit cell gives rise to an infinitely extended straight chain of CH_4 molecules parallel to the tube axis inside or outside it. The nanotube thus works as a template for the creation of linear/zigzag chains or the circular tubes of CH_4 molecules.

It is known that the DFT theory both in the GGA and LDA takes into account only the short range interactions, namely the chemical ones. We call this calculated binding energy the CBE here. The DFT does not include the weak long range vdW interactions or the dispersion forces. In the case of the chemisorption of the reactive atoms or molecules, strong chemical binding exists and the small contribution of the vdW energy is often omitted. However, in the case of the physisorption of the inert or saturated atoms or molecules such as the CH_4 molecule, the contributions of both the short range and long range vdW interactions are comparable and in some cases the latter dominates and thus one has to consider both the contributions. For the physisorption of the inert CH_4 molecule on the carbon nanotubes, we include the attractive vdW interaction energy here by employing the relation

$$E_{\mathrm{vdW}} = -\sum_i \sum_j C_{ij} \left(\frac{1}{r_{ij}}\right)^6 \tag{1}$$

where C_{ij} is a parameter having the units as energy $\times$ (distance)^6 and the subscripts i and j stand for the CH_4 molecules and C atoms, respectively.

For the determination of the C_{ij} for the CH_4 molecule–CNT vdW interaction, we employ the values of C_{ij} for the atoms given by Halgren (1992) and use the combination relation within the Slater–Kirkwood approximation. C_{ij} is obtained as equal to 1353.0 eV (au)^6. In determining the vdW energy, we have checked the convergence of the calculated vdW energy by including more and more C atoms of the infinitely long carbon tube.

In a reliable quantitative estimation of BE, another parameter which needs to be considered is the zero-point vibrational energy (ZPVE) given by

$$E_{\mathrm{zp}} = \tfrac{1}{2} \sum_i \hbar\omega_i \tag{2}$$

where the sum is over all the phonon frequencies (ω_i) for all the atoms in an unit cell.

For the estimation of E_{zp}, a quite sophisticated calculation for the phonon dispersion curves and the density of phonon states has to be performed, which is beyond the scope of the present study. We use a simple method for the estimation of E_{zp}. We study the motion of the adsorbed CH_4 molecule along with all the nearest and next-nearest neighbouring atoms in the host tube, keeping the other host carbons stationary within an *ab initio* pseudopotential theory. We calculate the phonon energies at two symmetric points in the Brillouin zone (BZ), a point ($\vec{q} = 0, 0, 0$) lying at the centre of the BZ and another at the boundary of the BZ ($\vec{q} = 0, 0, 0.5$).

The frequencies of the modes have been computed and the averaged values have been taken. We denote the enhanced ZPVE for the doped tube over the sum of the ZPVEs of the undoped and the isolated CH_4 molecule chain by ΔE_{zp}. For its determination, we subtract the sum of the ZPVE of the undoped nanotube and the ZPVE of the isolated CH_4 chain from that of the doped nanotube. For obtaining the final BE, one has to subtract this increased zero-point energy ΔE_{zp} from the sum of the CBE and the vdW energies. The currently calculated values of ΔE_{zp} are significant. The ZPVE calculations have been possible for the exohedral adsorption. For the endohedral adsorption, the number of the neighbouring host C atoms is

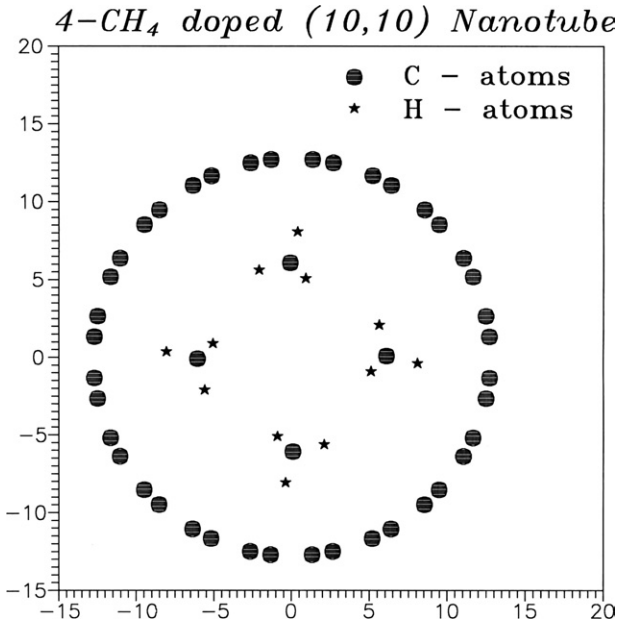

Figure 1. Atomic configuration of an optimized (10, 10) nanotube containing four CH_4 molecules inside the tube. All the atoms have been projected in one plane.

quite large and the calculation needs more advanced computation facilities beyond our reach. For the endohedral adsorption, we have, thus, chosen ΔE_{zp} as obtained for the case of the exohedral adsorption.

3. Calculation and results

3.1. Structural properties

We consider all the various stable configurations of the nanotubes with one or more than one CH_4 molecules per unit cell both inside and outside the tubes, separately. The CH_4 molecule lying on the off-tube axis location inside the tube or on the surface of the tube changes the point-group symmetry of the host tube. On the surface of the tube, the studied sites are the CH_4 molecule residing either above the mid point of a C–C bond (mid-bond) of the host tube or at the centre of the hexagon formed by six host C-atoms (mid-hexagon). As a typical case, we depict a (10, 10) nanotube containing four CH_4 molecules inside the tube in a plane normal to the tube axis in figure 1. Here, the host atoms projected only in one plane and the atoms of the CH_4 molecule lying in two planes have been shown.

The orientation of the CH_4 molecule has also been changed to achieve the minimum energy at each site of the nanotube. There are two symmetric axes, C_{3v} (along $\langle 111 \rangle$) and C_{2v} (along $\langle 110 \rangle$) for the CH_4 molecule and either of these symmetric axes may be either parallel or normal to the tube axis. Further, the system energy may also depend upon the rotation of the molecule about its own symmetric axis. During optimization, we have considered all such possibilities and determined the optimized BEs.

3.1.1. Small diameter nanotubes. We first investigate the three types of 4 Å diameter nanotubes, two achiral, the armchair (3, 3) and the zigzag (5, 0), and one chiral (4, 2) tube,

Table 1. Chemical binding energy in eV in LDA and GGA with different exchange–correlation functionals for the adsorption of one CH_4 molecule on the surface of the (3, 3) and (5, 0) carbon nanotubes for cut-off energies of 80 and 60 Ryd, respectively.

One CH_4 Surface		GGA	
mid-hexagonal site	LDA	PBE	BLYP
(3, 3)	0.065	−0.090	−0.087
(5, 0)	0.084	−0.041	−0.027

and study the chirality dependent effects of the adsorption on the tube. The diameters of the undoped, (5, 0), (3, 3) and (4, 2) nanotubes are 4.10, 4.34 and 4.28 Å, respectively. Thereafter, we extend our study to the larger diameter nanotubes like (10, 0) and (10, 10) to see the role of the large diameter in the adsorption. The diameters of the zigzag (10, 0) and the armchair (10, 10) nanotubes are 7.85 and 13.49 Å, respectively,

As the size of the CH_4 molecule is comparatively large for the small diameter 4 Å nanotube, its insertion inside any of the small diameter 4 Å nanotubes is not favoured. The calculated BEs are seen to be quite negative, ruling out any possibility of the endohedral adsorption of the CH_4 molecule inside the 4 Å tube.

Further, our calculation for a CH_4 molecule present on an interstitial site of a rope formed by three nanotubes gives a negative CBE which cannot be compensated by the positive vdW energy. Thus, the insertion of CH_4 molecules between the 4 Å nanotubes in a bundle is not seen.

We have also performed calculations for a CH_4 molecule per unit cell residing in a groove formed by the two surfaces of the small diameter 4 Å nanotubes of a nanorope containing four parallel tubes among themselves. Again, the calculated CBE turns out to be negative, which remains uncompensated by the positive vdW energy. Thus, this type of adsorption is not possible.

The CH_4 molecules adsorbed on the nanotubes themselves are practically not distorted. The changes in the bond lengths and the bond angles in the CH_4 molecules are quite small and lie within 1% and 2%, respectively.

We observe a radial deformation all along the length of the nanotube. This radial deformation or buckling is measured by the percentage of the difference between the maximum and minimum radii of the rope with respect to the averaged radius of the tube. We find that the armchair (n, n) tubes are comparatively more buckled as compared to the zigzag (n, 0) tubes where one finds quite small buckling. However, for the most stable configurations, the buckling for the armchair (n, n) tubes is within 3.7%. In the armchair tubes, the separation between the neighbouring CH_4 molecules along the tube axis is much smaller as compared to the zigzag (n, 0) tubes, resulting in large buckling.

Convergence of chemical binding energy. At first, we determine the CBEs both in LDA and GGA using the TM pseudopotential and observe its variation w.r.t. the different exchange and correlation functionals like those of Perdew *et al* (1996) (PBE) and of Becke (1988) (BLYP). The CBEs for one k-point for the adsorption of the CH_4 molecule on the (3, 3) and the (5, 0) nanotubes in the above three approximations are shown in table 1. One obtains positive values of CBE for the CH_4 molecule in LDA against negative values in the GGA, which points towards the over-binding of the CH_4 molecule in LDA as has also been observed in other cases like the adsorption of O_2 on nanotubes (Zhao *et al* 2002, Dag *et al* 2003). We thus perform most of the calculations only in the GGA unless stated otherwise.

Table 2. Variation of the chemical binding energy in eV with respect to k-points for one-CH_4-doped (3, 3) and (5, 0) carbon nanotubes for cut-off energies of 80 and 60 Ryd, respectively.

k-points	(3, 3) nanotube	(5, 0) nanotube
1	−0.169	−0.041
2	−0.161	−0.044
4	−0.161	−0.044
6	−0.161	

Table 3. Variation of chemical binding energy in eV with cut-off energy for one-CH_4-doped (3, 3), (5, 0), (10, 10) and (10, 0) carbon nanotubes for two k-points.

Cut-off energy (Ryd)	Small diameter tubes		Large diameter tubes	
	(3, 3)	**(5, 0)**	**(10, 0)**	**(10, 10)**
40		−0.365	−0.750	
60	−0.171	−0.044	−0.044	
80	−0.161	−0.044	−0.024	−0.196
90	−0.161	−0.044	−0.024	

Further, we observe that in the GGA, the CBEs obtained for the PBE and the BLYP exchange and correlation functionals are quite similar. We choose the PBE exchange and correlation functional for obtaining CBEs.

CH_4-doped (3, 3) nanotube. One CH_4: We investigate the convergence of CBE with the number of k-points in the BZ. The CBE converges within 2% with an increase in the number of k-points in the BZ. As an example, the values of CBE obtained for 1–6 k-points in the BZ for the surface adsorption of the CH_4 molecule on the (3, 3) and (5, 0) tubes are depicted in table 2.

The convergence of CBE with the cut-off energy of the plane waves was studied. We varied the cut-off energy from 40 to 90 Ryd and observe that the CBE converges for such a large cut-off energy variation. The computed CBEs for the several cut-off energies for the adsorption of the CH_4 molecule on the various tubes are shown in table 3. For all the tubes except the (5, 0) tube, the CBE converges at the cut-off energy of 80 Ryd.

The calculated ZPVEs for the (3, 3) nanotube doped with one CH_4 molecule on the mid-hexagonal site for the wavevectors $\vec{q} = (0, 0, 0)$ and (0, 0, 0.5) are 2816.6 and 2842.0 meV, respectively, whereas for the pristine tube these values are 1311.9 and 1394.5 meV, respectively. The ZPVE values for the isolated CH_4 molecule chain for $\vec{q} = (0, 0, 0)$ and (0, 0, 0.5) are 1395.5 and 1481.6 meV, respectively. After taking the averages for the two $\vec{q}$-points for each system, the enhanced zero-point energy, ΔE_{zp}, turns out to be 38 meV. A positive contribution means here that the ZPVE of the doped tube is larger than the sum of the ZPVEs of the undoped tube and the isolated CH_4 molecular chain, and it decreases the binding of the CH_4 molecule to the nanotube.

The final BEs (chemical BE + vdW energy − enhanced zero point energy) for the CH_4 molecule lying on the various sites of the various nanotubes, the averaged tube diameters, the averaged minimum separations between the host C atom and the C atom of the adsorbed CH_4 molecule and the tube buckling are shown in tables 4–8.

The CBEs in the GGA for the high concentrations of the CH_4 molecules (one CH_4 molecule per unit cell) on the surface of the (3, 3) nanotube as shown in table 4 are seen to be negative, lying in the range of −0.329 to 0.027 eV, indicating no adsorption. The binding

Table 4. Binding energies per CH_4 molecule in eV for the adsorption of a CH_4 molecule on (3, 3) nanotubes in the GGA. All the data are in the GGA except those written inside the brackets as the LDA. The final energy is equal to CBE + vdW energy − zero point energy (=0.038 eV). The averaged diameters of the tubes, the separation between the C of the CH_4 and the nearest C of SWNT in Å and the bucklings are also included.

Position of CH_4 molecule	CBE	vdW energy	Final BE	Tube diameter	CH_4–C separation	Buckling (%)
One CH_4 on one unit cell						
Surface mid-hexagon						
C_{2v}_symm_z_001	−0.161	0.169	−0.030	4.19	3.29	1.5
C_{2v}_symm_z_110						
rot_0	−0.125	0.147	−0.016	4.17	3.39	2.1
rot_45	**−0.090**	**0.149**	**0.021**	**4.17**	**3.37**	**2.2**
(LDA)	0.065	0.149	0.176	4.17	3.37	2.2
rot_90	−0.150	0.157	−0.031	4.17	3.37	2.7
C_{3v}_symm_z_111						
normal to tube axis						
3_H_away_from_tube	−0.155	0.159	−0.034	4.17	3.34	2.3
3_H_towards_tube						
rot_0	−0.155	0.159	−0.034	4.17	3.33	2.7
rot_60	−0.329	0.225	−0.142	4.17	3.11	7.8
parallel to tube axis	−0.144	0.157	−0.025	4.16	3.36	2.7
Surface mid-bond						
C_{2v}_symm_z_110						
rot_45	**−0.027**	**0.096**	**0.031**	**4.18**	**3.46**	**0.8**
(LDA)	0.060	0.096	0.118	4.18	3.46	0.8
One CH_4 on two unit cells						
Surface mid-bond						
C_{2v}_symm_z_110						
rot_45	**−0.024**	**0.103**	**0.041**	**4.19**	**3.42**	**1.2**
One CH_4 Groove-site	Unstable					
One CH_4 Interstitial between 3 tubes	Unstable					

is caused by the vdW energy. For specific orientations of the CH_4 molecule, the final BEs for the mid-bond and the mid-hexagonal surface sites are only 0.031 and 0.021 eV, respectively, which are quite small. On the other hand, the corresponding LDA values are quite large, equal to 0.118 and 0.176 eV for the mid-bond and the mid-hexagonal surface sites, respectively. The averages of the CBE values obtained in the GGA and LDA for the mid-bond and the mid-hexagonal surface sites are 0.017 and −0.013 eV, respectively, whereas the vdW energies for the two types of sites are 0.096 and 0.149 eV, respectively. One may, thus, observe that the vdW energy is either of the same order as the CBE or about double the CBE.

One CH_4 molecule per unit cell containing 12 C atoms will give rise to a concentration of 8.3%. For the mid-bond site, we reduced this concentration to half (4.2%) by optimizing the configuration where there is one CH_4 molecule for two unit cells. The BE increases to 0.041 eV, an enhancement of about 33%. The CH_4–C distance for this configuration is reduced only by 1.0% and the induced buckling increases to 1.2%. One may expect further small enhancement of BE for smaller concentrations of the CH_4 molecules and a small adsorption of the CH_4 molecules in practice.

Table 5. Binding energies per CH_4 molecule in eV for the adsorption of CH_4 molecules on (5, 0) nanotubes in the GGA. All the data are in the GGA except those written inside the brackets as the LDA. The final energy is equal to CBE + vdW energy − zero point energy (=0.031 eV). The averaged diameters of the tubes, the separation between C of CH_4 and the nearest C of SWNT in Å and the bucklings are also included.

Position of CH_4 molecule	CBE	vdW energy	Final BE	Tube diameter	CH_4–C separation	Buckling (%)
One CH_4 on one unit cell						
Surface mid-hexagon						
C_{2v}_symm_z_001	−0.044	0.107	0.032	4.09	3.49	0.2
C_{2v}_symm_z_110						
rot_0	**−0.041**	**0.107**	**0.035**	**4.09**	**3.49**	**0.2**
rot_45	−0.052	0.107	0.024	4.09	3.49	0.2
C_{3v}_symm_z_111						
normal to tube axis						
3_H_away_from_tube	**−0.041**	**0.107**	**0.035**	**4.09**	**3.49**	**0.2**
(LDA)	0.090	0.107	0.166	4.09	3.49	0.2
3_H_towards_tube						
rot_0	−0.065	0.106	0.010	4.07	3.50	0.4
rot_60	−0.063	0.106	0.012	4.08	3.50	0.3
parallel to tube axis	−0.071	0.106	0.004	4.08	3.49	0.3
Surface mid-bond						
C_{2v}_symm_z_110						
rot_0	−0.109	0.135	−0.005	4.06	3.22	3.7
C_{3v}_symm_z_111						
normal to tube axis						
3_H_away_from_tube	−0.112	0.137	−0.006	4.07	3.21	3.1
One CH_4	Unstable					
Groove site						
One CH_4	Unstable					
Interstitial						
between three tubes						

Table 6. Binding energy per CH_4 molecule in eV for the adsorption of CH_4 molecules on (4, 2) nanotubes. The final energy is equal to CBE + vdW energy − zero point energy (=0.031 eV). The averaged diameters of the tube, the separation between the C of CH_4 and C of SWNT in Å and the buckling are also included.

Position of CH_4 molecule	CBE	vdW energy	Final BE	Tube diameter	CH_4–C separation	Buckling (%)
One CH_4 on one unit cell						
Surface mid-bond						
C_{2v}_symm_z_110	−0.493	0.305	−0.219	4.29	2.73	4.3
One CH_4						
Groove-site	Unstable					
One CH_4						
Interstitial	Unstable					
between 3 tubes						

The lattice constant for one unit cell for the (3, 3) tube along the tube axis is 2.39 Å. As this separation of 2.39 Å between the two CH_4 molecules along the chain formed along the

Table 7. Binding energy per CH_4 molecule in eV for the various concentrations of adsorption of CH_4 molecules in or on (10, 0) nanotubes in the GGA. All the data are in the GGA except those written inside the brackets as the LDA. The final energy is equal to CBE + vdW energy − zero point energy (=0.071 eV). The averaged diameters of the tubes, the separation between the C of CH_4 and C of SWNT in Å and the bucklings are also included.

Position of CH_4 molecule	CBE	vdW energy	Final BE	Tube diameter	CH_4–C separation	Buckling (%)
One CH_4						
Inside						
C_{2v}_symm_z_110						
rot_0	**−0.014**	**0.352**	**0.267**	**7.86**	**3.99**	**0.1**
(LDA)	0.280	0.352	0.561	7.86	3.99	0.1
C_{3v}_symm_z_111						
normal to tube axis	−0.022	0.349	0.256	7.86	3.99	0.1
parallel to tube axis	−0.014	0.349	0.264	7.86	4.00	0.1
One CH_4						
Surface mid-hexagon						
C_{2v}_symm_z_001	−0.024	0.103	0.008	7.86	3.65	0.0
C_{2v}_symm_z_110						
rot_0	−0.027	0.103	0.005	7.86	3.65	0.0
rot_45	**−0.016**	0.103	**0.016**	**7.86**	**3.65**	**0.0**
(LDA)	0.082	0.103	0.114	7.86	3.65	0.0
C_{3v}_symm_z_111						
normal to tube axis						
3H_away_from_tube	−0.019	0.103	0.013	7.86	3.65	0.0

Table 8. Binding energy per CH_4 molecule in eV for the various concentrations of adsorption of CH_4 molecules in or on (10, 10) nanotubes. The final energy is equal to CBE + vdW energy − zero point energy (=0.039 eV). The averaged diameters of the tubes, the separation between the C of CH_4 and C of SWNT in Å and the bucklings are also included.

Position of CH_4 molecule	CBE	vdW energy	Final BE	Tube diameter	CH_4–C separation	Buckling (%)
Four CH_4 on one unit cell						
Inside						
C_{2v}_symm_z_110						
rot_45	**−0.047**	**0.166**	**0.080**	**13.50**	**3.62**	**0.1**
(LDA)	0.079	0.166	0.206	13.50	3.62	0.1
One CH_4 on one unit cell						
Surface mid-hexagon						
C_{2v}_symm_z_110						
rot_45	**−0.196**	**0.232**	**−0.003**	**13.50**	**3.21**	**3.7**
(LDA)	0.024	0.232	0.217	13.50	3.21	3.7
C_{3v}_symm_z_111						
parallel to tube axis	−0.305	0.257	−0.087	13.50	3.14	3.0
Surface mid-bond						
C_{2v}_symm_z_110						
rot_45	−0.204	0.230	−0.013	13.50	2.97	3.6

tube axis is smaller than the equilibrium separation of 3.28 Å between the two CH_4 molecules in an isolated chain, there is some positive (repulsive) contribution to the energy of the doped tube because of the CH_4–CH_4 interactions. This adsorbate–adsorbate interaction vanishes for low concentration of the CH_4 molecules.

A perusal of table 4 reveals that the changes induced by the CH_4 molecule in the averaged diameter of the (3, 3) tube are again less than 4%. The buckling is quite small for the mid-bond site. In general, the buckling induced by the CH_4 molecules in the (3, 3) tube is large as compared to that for the (5, 0) tube, as will be seen later.

It has been observed that the isolated CH_4 molecular linear chain that is adsorbed on the (3, 3) nanotube is unstable, as it has negative chemical binding energy with respect to the single CH_4 molecule. The CH_4 molecular chain is stabilized by the underneath carbon nanotube.

CH_4-doped (5, 0) nanotube. One CH_4: The convergence of CBE with the number of k-points in BZ has been checked and the results are shown in table 2. We find the convergence of CBE at the cut-off energy of 60 Ryd as shown in table 3.

The calculated E_{zp} values for one CH_4 molecule adsorbed on the mid-hexagonal site of the (5, 0) nanotube at $\vec{q} = (0, 0, 0)$ and (0, 0, 0.5) points are 2217.5 and 2292.8 meV, respectively, whereas for the pristine tube these values are 797.7 and 874.8 meV, respectively. The E_{zp} values for the isolated CH_4 molecular chain for $\vec{q} = (0, 0, 0)$ and (0, 0, 0.5) are 1351.6 and 1424.7 meV, respectively. An average of the values at the two q-points gives an enhanced zero-point energy, ΔE_{zp}, equal to 0.031 eV after the adsorption. A positive contribution means that the ZPVE of the doped tube is larger than the sum of the ZPVEs of the undoped tube and the isolated CH_4 molecule and it reduces the binding of the CH_4 molecule to the nanotube.

The final BEs for the (5, 0) tube doped with one CH_4 molecule per unit cell on the surface are quite similar to those of the (3, 3) tube. A maximum BE of 0.035 eV is seen for a CH_4 molecule residing at the mid-hexagonal site of the (5, 0) tube for the two different orientations of the CH_4 molecule, as has been shown in table 5. In these configurations, the tube axis is either parallel to the C_{2v}- or C_{3v}-fold symmetric axis of the CH_4 molecule. The final BEs for the mid-bond sites are practically zero.

The lattice constant for the (5, 0) tube along the tube axis is 4.23 Å and is greater than the equilibrium separation of 3.28 Å between the two CH_4 molecules in the chain kept in vacuum; there is no significant contribution of the CH_4–CH_4 interactions to the energy of the doped tube. In fact, the CH_4 molecular chain residing on the (5, 0) tube in isolation is again unstable and is stabilized by the host tube.

One CH_4 molecule per unit cell corresponds to an adsorbate concentration of 5%. We thus expect small adsorption of CH_4 molecules on the (5, 0) tube.

A perusal of table 5 reveals that the changes induced by the CH_4 molecules in the averaged diameter of the tube are very small and are less than 1%. The variation in the minimum separation between the C atom of the host tube and the C atom of the CH_4 molecule is appreciable and is within 8%. On the other hand, the buckling induced by the CH_4 molecules in the various most stable CH_4-(5, 0) nanotube configurations is negligible.

The LDA value for the CBE for one CH_4 adsorbed site is 0.090 eV. The average of the LDA and GGA CBEs is 0.025 eV. One observes that the average is positive but quite small in magnitude. The vdW energy is 0.107 eV which is more than four times of the CBE.

CH_4-doped (4, 2) nanotube. For the (4, 2) nanotube (see table 6), the BE in GGA for one CH_4 molecule residing on the mid-bond site is negative (BE $= -0.219$ eV) indicating no adsorption. The changes induced by the CH_4 molecules in the averaged diameter of the (4, 2) tube is negligible. The radial distortions (buckling of 4.3%) induced by the adsorbed CH_4 molecules are comparable with the other 4 Å (3, 3) nanotube. The C of CH_4 and host C minimum separation of 2.73 Å is smaller as compared to a separation of 3.4 Å seen in the other 4 Å tubes. Calculation for the enhanced zero-point energy, ΔE_{zp}, was not done and a value of $\Delta E_{zp} = 0.031$ eV obtained earlier for the (5, 0) was chosen.

3.1.2. Large diameter nanotubes

CH_4-doped (10, 0) nanotube. The convergence of CBE both with the number of k-points in the BZ and the plane wave cut-off energy has been checked. Table 3 contains the results of the convergence with respect to the plane wave cut-off energy. The convergence of CBE is seen at the cut-off energy of 80 Ryd.

For the surface mid-hexagonal site adsorption, E_{zp} values for the doped tube for $\vec{q} = (0\ 0\ 0)$ and $(0\ 0\ 0.5)$ are 2661.0 and 2779.2 meV, respectively. For the undoped tube, E_{zp} values are 1216.8 and 1305.5 meV for $\vec{q} = (0\ 0\ 0)$ and $(0\ 0\ 0.5)$, respectively, and the corresponding values for the isolated CH_4 chain are 1342.5 and 1433.8 meV, respectively. ΔE_{zp} turns out to be quite appreciable equal to 71 meV. This value of ΔE_{zp} for the zigzag (10, 0) tube is much higher as compared to those obtained for the armchair (n, n) tubes.

In a comparatively wide achiral zigzag (10, 0) nanotube, the endohedral adsorption of a CH_4 molecule is possible, and as shown in table 7 the BEs for the different orientations of the CH_4 molecule are positive and comparatively quite high (approximately 0.26 eV). The BEs are quite the same for the CH_4 molecule residing inside the tube either in the plane of host C atoms or between the two planes of the C atoms of the tube. This will result in a smooth motion of the CH_4 molecule inside the (10, 0) nanotube without facing any potential barrier.

For the adsorption of the CH_4 molecule on the mid-hexagonal surface sites, the BE is seen to be positive but quite small (=0.016 eV) and is smaller as compared to that of the (5, 0) tube. The tube diameter of the (10, 0) tube remains unchanged after the adsorption of the CH_4 molecules. The minimum separation between the tube and the C atom of the CH_4 molecule (3.65 Å) is higher as compared to that of the 4 Å nanotubes (2.7–3.4 Å). The buckling is found to be quite small, lying within 0.1%.

Our LDA value of CBE equal to 0.082 eV is smaller than the value, 0.190 eV, reported by Zhao *et al* (2002). The earlier authors have performed calculations for a plane wave cut-off energy of 56 Ryd, whereas the present value has been obtained for a cut-off energy of 80 Ryd after achieving convergence for the cut-off energy as well as for the number of k-points chosen in the BZ. In table 7, we also include the LDA values of CBE both for the endohedral and exohedral adsorptions. The averages of the GGA and LDA CBEs for the endohedral and exohedral adsorptions are 0.133 and 0.033 eV, respectively. The corresponding vdW energies are 0.352 and 0.103, respectively. Again, one finds that the vdW contributions to BEs are about three times higher.

As the unit cell of the (10, 0) tube contains 40 C atoms, one CH_4 molecule in the unit cell corresponds to an adsorbate concentration of 2.5%, but in reality the adsorption concentration will be much smaller. For the strong endohedral adsorption, on the other hand, the adsorption concentration will be 2.5%.

CH_4-doped (10, 10) nanotube. The convergence of CBE both with the number of k-points in the BZ and the cut-off energy has been checked. The results for the convergence with the cut-off energy are shown in table 3 and one finds the convergence at the cut-off energy of 80 Ryd.

The approximate E_{zp} values for the doped tube for the adsorption on the surface mid-hexagonal site for $\vec{q} = (0\ 0\ 0)$ and $\vec{q} = (0\ 0\ 0.5)$ are 2813.0 and 2982.6 meV, respectively. The corresponding E_{zp} values for the undoped tubes are 1335.5 and 1495.4 meV, and those for the isolated CH_4 chain are 1410.0 and 1478.2 eV, respectively. These data give us the enhanced zero point energy, ΔE_{zp}, equal to 0.038 eV. In order to check the adsorption site dependence of ΔE_{zp}, we performed a similar calculation for the adsorption on the surface mid-bond site. A value of $\Delta E_{zp} = 0.041$ eV is obtained for the adsorption on the surface mid-bond site.

We, thus, observe that the enhanced zero point energies are quite similar for the surface mid-hexagonal and mid-bond sites.

Endohedral adsorption. In the wide achiral armchair (10, 10) nanotube, endohedral adsorption of a large number of CH_4 molecules is expected. We, therefore, consider four CH_4 molecules lying at the off-axis positions in an unit cell and observe a BE of 0.080 eV (table 8). It will lead to a maximum endohedral adsorbate concentration of 10%. The BEs are again quite similar for the CH_4 molecule residing inside the tube lying either in the plane of the host C atoms or between the two planes of the C atoms of the tube. Here, each CH_4 molecule lies 3.21 Å away from the axis. The CH_4–CH_4 molecular separation inside the tube is seen to be 4.54 Å which is larger than the corresponding separation of 3.28 Å between the molecules in the stable isolated chain and, therefore, no CH_4–CH_4 interaction will be seen. The minimum separation between the C atom of the CH_4 molecule and the host C atom is seen to be 3.62 Å for one or four adsorbed CH_4 molecules. The buckling is negligible.

Exohedral adsorption. The binding is quite weak for the exohedral adsorption. The CBEs for the exohedral adsorption are negative on all the different sites, similar to the small diameter (3, 3) tube. As shown in table 8, the BE is larger ($=-0.003$ eV) for the surface mid-hexagonal site of the CH_4 molecule when its twofold symmetric axis is parallel to the tube axis.

The BE for the surface mid-bond site is -0.013 eV, and therefore there exists a small potential barrier of 10 meV for the motion of the CH_4 molecule on the surface of the tube. This observed smoothness of the (10, 10) tube for the motion of the CH_4 molecule will lead to rapid transport of CH_4 gas along the tube as has been observed in experiments on some gases and in atomistic simulation too (Kleinhammes *et al* 2003).

We decreased the adsorbate concentration by placing one CH_4 molecule on the surface mid-hexagonal site of the two unit cells (80 atoms) and find that the BE somewhat increases to 0.002 eV. This will correspond to an adsorption concentration of 1.25% on the surface.

The averages of the CBEs in the GGA and LDA for the endohedral and the exohedral adsorption are 0.016 and -0.086 eV, respectively. On the other hand, the corresponding vdW energies are 0.166 and 0.232 eV, respectively. The vdW contributions are thus the dominant ones in the binding of the CH_4 molecule.

The diameter of the (10, 10) tube remains quite unchanged after the adsorption of the CH_4 molecules. The radial distortions (buckling) for the exohedral adsorption is appreciable, about 3.7%, similar to the (3, 3) nanotube.

The endohedral adsorption of the CH_4 molecules is much larger than that of the exohedral adsorption. The calculated maximum concentrations of the endohedral and exohedral adsorption of the CH_4 molecules are 2.5% and 1.25–2.5%, respectively. The experimental variation of the isosteric heat of adsorption q_{st} observed only for the closed tubes, i.e. for the exohedral adsorption of the CH_4 molecules, with the coverage has been computed from the available measured data (Weber *et al* 2000, Talapatra *et al* 2000) by Shi and Johnson (2003). The experimental values of q_{st} lie mainly in three concentration regions and the values are 0.282 eV for about 0.35% concentration, 0.166 eV for 1% concentration and 0.124 eV for 2% concentration, respectively. The highest value of q_{st} in the lowest concentration region has been assigned to the adsorption into the groove sites of the bundles of heterogeneous SWNTs having different diameters (Shi and Johnson 2003). The higher coverages are assigned to the surface adsorption. The binding energy is determined by the relation $\mathrm{BE} = q_{st} - 2k_BT$. At 70 K, for an experimental average value of q_{st} equal to 0.145 eV measured for the 1.5% concentration of adsorption, the BE turns out to be about 0.133 eV. For 1.5% adsorption, the present values

of BEs are −0.002 eV and 0.218 eV in the GGA and LDA, respectively, and their average is 0.108 eV, which is quite close to the experimental BE of 0.133 eV. Thus, the experimental BE lies between the LDA and GGA values and an average of the computed values in the two approximations seems to be in reasonable agreement with the experimental value. One may thus infer that whereas the LDA over-binds the CH_4 molecule the GGA under-binds it, and for making a reliable theoretical estimate an average of the BEs determined in the LDA and GGA may be good.

A perusal of tables 4–8 reveals that there is no obvious correlation between the BEs either with the tube diameters or with the minimum separation between the C of CH_4 molecule and that of the host tube.

In the present study, one-dimensional chains of the adsorbed CH_4 molecules have been considered because of the periodic repetition of the supercells. In reality or in practice, the molecules may be adsorbed on random positions which do not form the chains and thus the wavevector is a bad quantum number. In this case the obtained wavevector energy dependence for the CH_4 molecules will not be valid. For a low concentration of the molecules, the molecule–molecule interactions are negligible and the present results would be valid for the adsorption of one molecule on the tube. One can simulate the random adsorption of the molecules, equivalent to the adsorption of a single molecule, and the present results are applicable to the random adsorption except the transport properties. The random potentials created by the adsorbates will produce quasibonding states and will affect the transport properties of the tubes. On the other hand, a periodic arrangement of a high concentration of the adsorbed molecules will lead to adsorbate–adsorbate interactions causing dispersion in the hybridized CH_4–host C states which have been considered in the present study. However, the study of a random adsorption of a high concentration of the molecules on the tubes is beyond the present study.

3.2. Electronic structure

The electronic structure and the electron density of states (DOS) have been calculated for 26, 26, 16, 21 and 21 k-points chosen along the k_z-direction in the BZ for the (3, 3), (5, 0), (4, 2), (10, 0) and (10, 10) nanotubes, respectively. The DOS is computed with a broadening of 0.055 eV. The Fermi level (E_F) or the highest occupied state has been chosen as the origin of energy. For DOS, the full units are states/eV/unitcell, and for brevity in our further discussion we will write units instead of the full units.

For the DOS plots, it may be pointed out that our choice of a practically possible grid of the k-points in the BZ generates some spurious spiky structures. The peaks appearing in the DOS arising from the occurrence of the vHss in the electronic structure are the only correct ones and other wavy or spiky features are artifacts of the calculation and should be ignored.

CH_4-doped (3, 3) nanotube. The electronic structure and the DOS for the pristine (3, 3) nanotubes are presented in figure 2(a). The bonding and the anti-bonding (24, 25) states cross at E_F (named Δ_F) and the tube is metallic, as expected by symmetry considerations. The DOS at E_F is 0.31 units. In figure 2(a), we have shown the highest occupied single 24th state and the lowest unoccupied single 25th state before the crossing point Δ_F ($k_z = 0.3$). For $k_z > 0.4$, we also depict the doubly degenerate occupied (23, 24) states and the doubly degenerate unoccupied (25, 26) states which have come up (down) in the valence (conduction) band region with respect to the bonding–antibonding pair (24, 25) before $k_z = 0.35$. These states contain two saddle points near the boundary of the BZ in the vicinity of E_F. In fact, these states are seen to contribute to optical transitions and have been shown in figure 2(a).

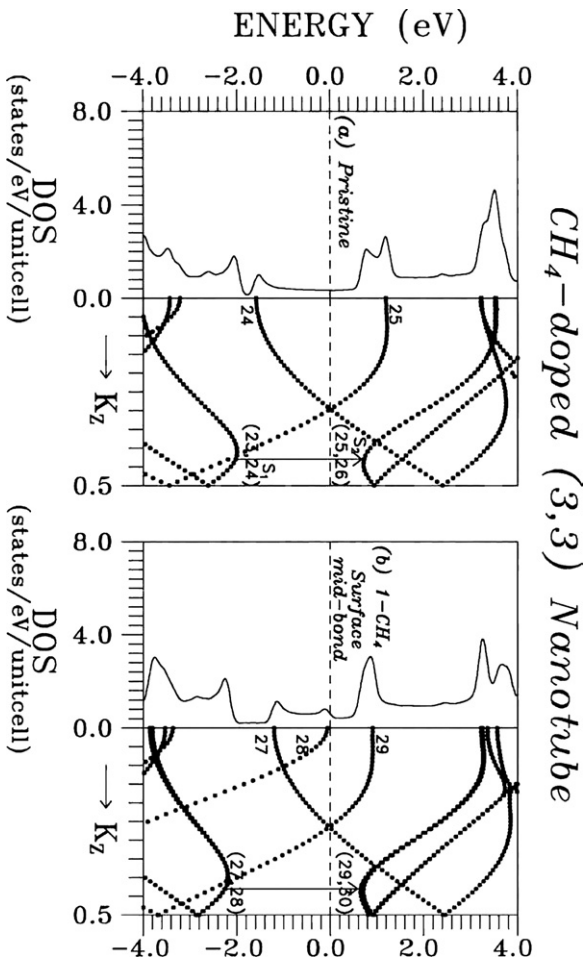

Figure 2. Electronic structure and the density of electron states in the vicinity of the Fermi level for the (3, 3) nanotube: (a) pristine, (b) one CH_4 molecule on surface mid-bond site. The doubly degenerate topmost filled and the lowest unfilled states have been marked as (23, 24) and (25, 26) near the BZ boundary for the pristine tube. The numbering is different at various values of k_z. Some typical optical transitions have also been depicted.

One CH_4. The electronic structure and the DOS for the CH_4 molecule residing on the surface mid-bond site of the (3, 3) tube are presented in figure 2(b). The electronic structure is changed in the neighbourhood of E_F. This is the consequence of the breaking of the symmetry of the host tube by the CH_4 molecule residing on the surface. Although the crossing of the bonding–antibonding carbon states is not disturbed, one low lying valence state gets mixed with the states of the CH_4 molecule and incurs splitting. In the vicinity of E_F, all the states are the hybridized C(p)–H(s, p) ones. Almost all the states lying in the valence and conduction band regions split. The DOS is enhanced considerably from 0.31 units seen for the pristine tube to 1.08 units for the mid-bond site. For the details, the states in the vicinity of E_F have been numbered and some optical transitions have been shown in figure 2(b) for later discussion.

CH_4-doped (5, 0) nanotube. The pristine (5, 0) tube is expected to be semiconducting by symmetry considerations. However, because of the strong curvature effects, a state 'α' lying

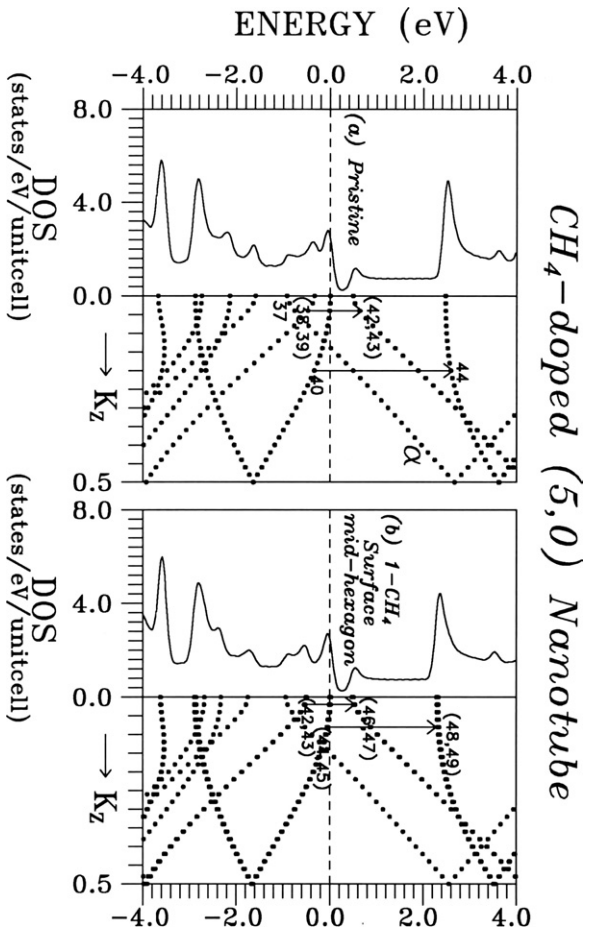

Figure 3. Electronic structure and the density of electron states in the vicinity of the Fermi level for the (5, 0) nanotube: (a) pristine and (b) one CH_4 molecule on the surface-mid-hexagonal site. For the pristine tube, the doubly degenerate topmost filled and the lowest unfilled states have been marked as (38–40) and (42–44) near the centre of the BZ. The numbering is different at various values of k_z. Some typical optical transitions have also been demonstrated.

in the conduction band region next to E_F descends quite appreciably and makes the nanotube conducting (figure 3(a)). A van Hove singularity (vHs) from the valence band region touches E_F and enhances the DOS to 2.48 units. The next conduction state lies about 0.5 eV higher at $k_z = 0$. In figure 3(a) we have numbered the states in the neighbourhood of E_F and have also shown some optical transitions.

One CH_4. The electronic structure and DOS for one CH_4 lying above the mid-hexagonal site of the host C-atom of the (5, 0) nanotube is presented in figure 3(b). A number of the states lying in the vicinity of the E_F split. Among them, the α state and the uppermost doubly degenerate valence state which cross just below E_F split. One of the split valence states rises regularly and crosses E_F. The other one bends downwards. The α state also bends but upwards. This is the consequence of the breaking of the symmetry of the host tube by the CH_4 molecule residing on the surface. The DOS for the doped tube at E_F is 2.44 units, in contrast to a value

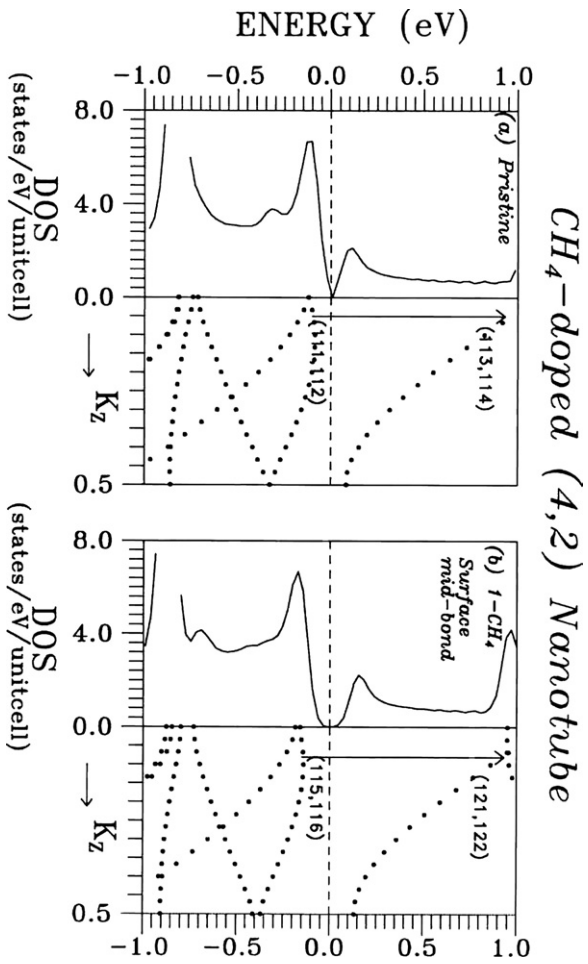

Figure 4. Electronic structure and the density of electron states in the vicinity of the Fermi level for the (4, 2) nanotube in a smaller energy range of −1.0–1.0 eV: (a) pristine; (b) one CH_4 molecule on surface mid-bond site. For the pristine tube, the doubly degenerate topmost filled and the lowest unfilled states have been marked as (111–112) and (113–114) near the centre of the BZ. Some typical optical transitions have also been shown.

of 2.48 units for the pristine tube, and thus remains unaltered by the adsorption of the CH_4 molecule. The states in the vicinity of E_F for the pristine tube have been numbered and some optical transitions are shown in figure 3(b).

CH_4-doped (4, 2) nanotube. The pristine (4, 2) nanotube is semiconducting and its electronic structure and DOS are shown in figure 4(a). The electronic structure and DOS for one CH_4-doped (4, 2) nanotube are presented in figure 4(b). In a bid to see clearly the occurrence of the small indirect energy gaps, in figure 4 we have depicted the blown-up results only in the energy interval −1.0–1.0 eV, in contrast to the other results presented in the energy interval of −4.0 to 4.0 eV for the other nanotubes. The incorporation of CH_4 molecule on the surface of the (4, 2) nanotube does not make any significant change in the electronic structure of the pristine (4, 2) tube in the vicinity of E_F as the tube has quite low symmetry. The valence and the conduction

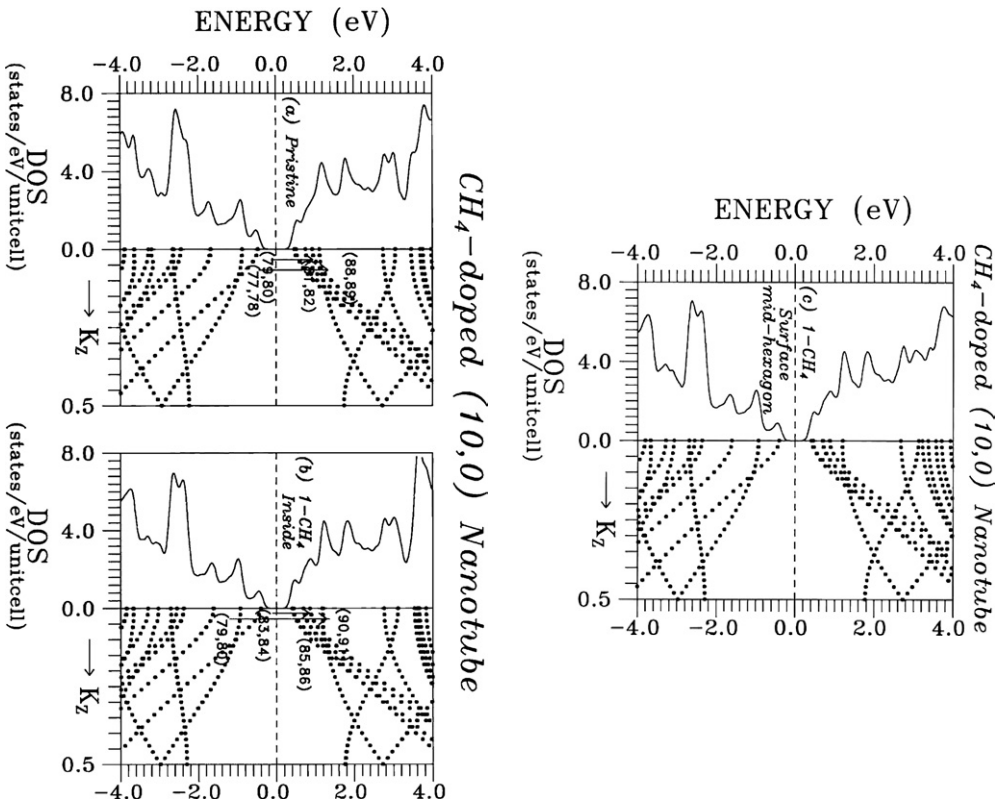

Figure 5. Electronic structure and the density of electron states in the vicinity of the Fermi level for a (10, 0) nanotube: (a) pristine, (b) one CH_4 molecule inside the tube and (c) one CH_4 molecule on the surface mid-hexagonal site. The doubly degenerate topmost filled and the lowest unfilled states have been marked as (77, 78) and (81, 82) near the centre of the BZ for the pristine tube. Some typical optical transitions have also been demonstrated.

states move away from E_F, resulting in the enhancement of the indirect bandgap from 0.17 to 0.29 eV for one CH_4 molecule. Chang *et al* (2004) have also reported an indirect energy gap of similar order for the pristine (4, 2) tube.

In figure 4, for the pristine and the doped tubes the states near E_F have been numbered and some optical transitions have been shown for later discussion.

CH_4-doped (10, 0) nanotube. The pristine (10, 0) tube is semiconducting as expected by symmetry considerations (figure 5(a)). No conduction state has descended into the gap, in contrast to a situation seen earlier for the large curvature (5, 0) nanotube. The magnitude of the semiconducting gap is 0.93 eV. For details, some of the states in the vicinity of E_F involved in the two lowest energy optical transitions have been numbered, which will be discussed later.

One CH_4. The electronic structure and DOS for one CH_4-doped (10, 0) nanotube for the CH_4 molecule lying inside the nanotube and at the surface mid-hexagonal site of the host C-atom are presented in figures 5(b) and (c), respectively. The above quantities are quite the same for all types of the endohedral and the exohedral adsorption of the CH_4 molecules. A number of the conduction states lying in the vicinity of the E_F descend towards E_F and the bandgap is

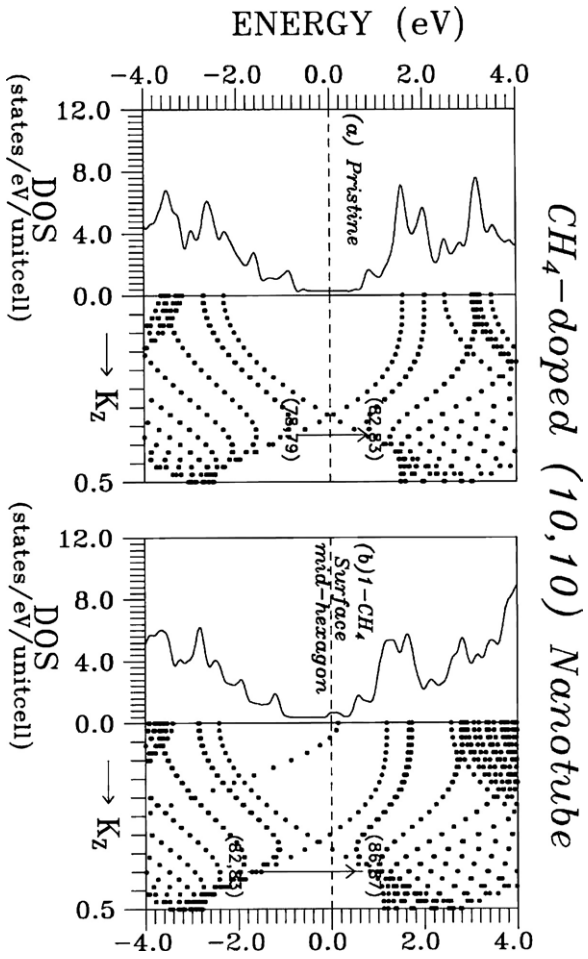

Figure 6. Electronic structure and the density of electron states in the vicinity of the Fermi level for the (10, 10) nanotube: (a) pristine and (b) one CH_4 molecule on the surface mid-hexagonal site. For the pristine tube, the doubly degenerate topmost filled and the lowest unfilled states have been marked as (78, 79) and (82, 83) near the boundary of the BZ. Some typical optical transitions have also been drawn.

reduced to 0.81 eV. We number some states in the vicinity of E_F and depict some transitions in figures 5(a) and (b).

CH_4-doped (10, 10) nanotube. The electronic structure and the DOS for the pristine achiral armchair (10, 10) nanotube are presented in figure 6(a). The bonding and the anti-bonding (80, 81) states cross at $k_z = 0.35$ (Δ_F) and the tube is metallic as expected by symmetry considerations. The two saddle points observed near the boundary of the BZ in the vicinity of E_F appear for $k_z < \Delta_F$ in contrast to the (3, 3) nanotube, where they were seen to occur for $k_z > \Delta_F$. In figure 6(a), we have shown the highest occupied single 80th state and the lowest unoccupied single 81st state and the optical transition. The DOS at E_F is 0.25 units.

One CH_4. The electronic structure and the DOS for the CH_4 molecule residing on the surface mid-hexagonal site of the (10, 10) nanotube are presented in figure 6(b). The

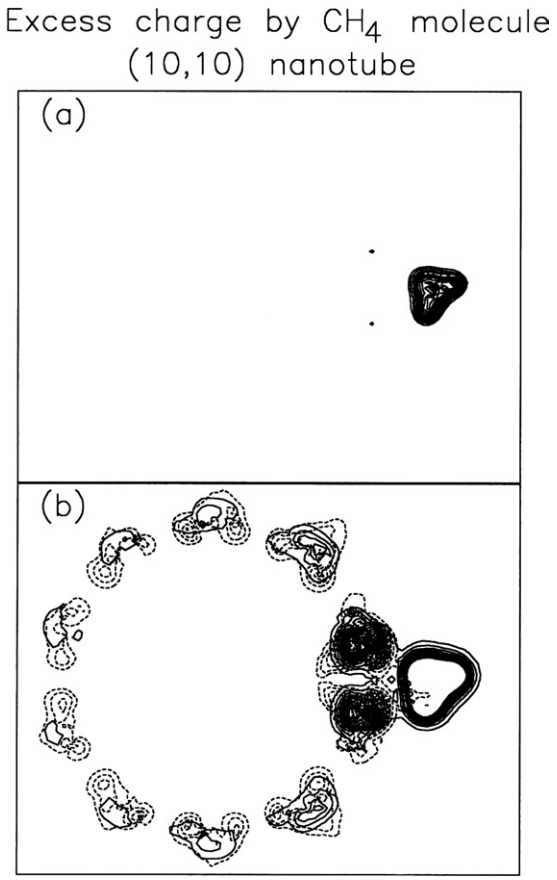

Figure 7. The excess electronic charge on the (10, 10) nanotube containing one CH_4 molecule over the pristine tube. The charge contours are shown in the range of (a) 0.054–0.30 e au^{-3} with an interval of 0.02 e au^{-3} and (b) 0.00–0.052 e au^{-3} with an interval of 0.004 e au^{-3}.

electronic states are quite the same for all types of endohedral and exohedral adsorption. The electronic structure is not much changed in the neighbourhood of E_F. The crossing of the bonding–antibonding carbon states descends below E_F, and similar to the (3, 3) nanotube one low lying valence states rises and mixes with the states of the CH_4 molecule. In the vicinity of E_F, the states are now the hybridized C(p)–H(s, p) ones. The states both in the conduction and valence bands split and give rise to more peaks in DOS. The value of DOS is enhanced considerably from 0.25 units seen for the pristine tube to 0.86 units. Some states near E_F are numbered in figure 6(a). Optical transition has also been depicted in the figure.

The electronic charge density plots of the CH_4 adsorbed nanotubes reveal a quite weak bonding between the CH_4 and the host nanotube. In figure 7, we depict the excess electronic charge on the doped tube over the pristine tube in one C-plane of the (10, 10) nanotube possessing one CH_4 molecule outside the tube. In figure 7(a) the charge contours are shown in the range of 0.054–0.30 e au^{-3} with an interval of 0.02 e au^{-3}, and in figure 7(b) in the range 0.00–0.052 e au^{-3} with an interval of 0.004 e au^{-3}. The solid lines depict the excess charge, whereas the dashed lines depict the depleted charge.

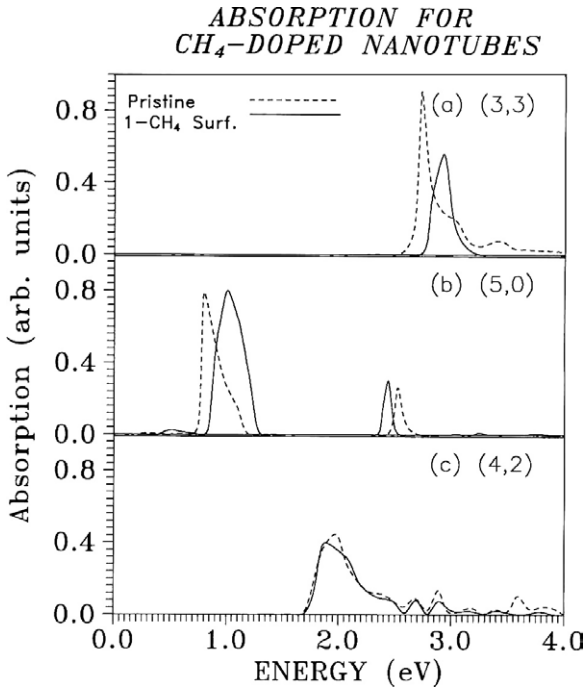

Figure 8. Absorption spectra for the pristine and the CH_4-molecule-doped (a) (3, 3), (b) (5, 0) and (c) (4, 2) nanotubes in the energy range of 0–4.0 eV, respectively.

3.3. Optical absorption

We calculate the optical absorption spectra of the isolated nanotube and the CH_4 doped tubes by using the absorption coefficient as (Hybertson and Needles 1993)

$$\alpha(\omega) = \frac{4\pi^2 e^2}{ncm^2\omega V_c} \sum_{v,c,\vec{k}} \left|\vec{\varepsilon} \cdot \vec{p}_{cv}(\vec{k})\right|^2 \delta\left(E_c - E_v - \hbar\omega\right). \tag{3}$$

Here m and e are the electron mass and charge, respectively. c is the velocity of light and n is the refractive index. V_c is the unit cell volume including the empty space. $\vec{\varepsilon}$ denotes a unit electric vector of the incident polarized light. For the wavevector $\vec{k}$, the conduction and the valence state energies are denoted by E_c and E_v, respectively. The momentum operator matrix element $\vec{p}_{cv}(\vec{k})$ is given by

$$\vec{p}_{cv}\left(\vec{k}\right) = \left\langle \psi_c, \vec{k} \middle| \vec{p} \middle| \psi_v, \vec{k} \right\rangle \tag{4}$$

Here ψ_c and ψ_v denote the wavefunctions of the conduction and the valence states, respectively. The momentum operator is denoted by $\vec{p}$.

In the actual calculation, for simplicity, we confine the polarization of light in one Cartesian direction x, y or z only. Also a broadening of 0.1 eV has been used to remove the spiky structure arising from our choice of a coarse grid in the BZ to cope with the limited memory of the computer available to us.

The no-phonon optical absorption for the incident electromagnet polarization along the tube axis obtained for the various CH_4 molecule–tube configurations is compared with the pristine tubes in figures 8–10. In all cases, the absorption normal to the axis of each nanotube is quite small.

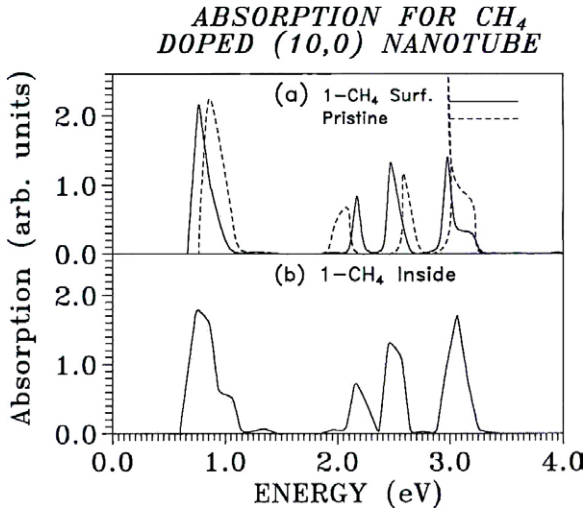

Figure 9. Absorption spectra in the energy range of 0–4.0 eV for the (10, 0) nanotube: (a) pristine and one CH_4 molecule on surface site, and (b) one CH_4 molecule inside the tube.

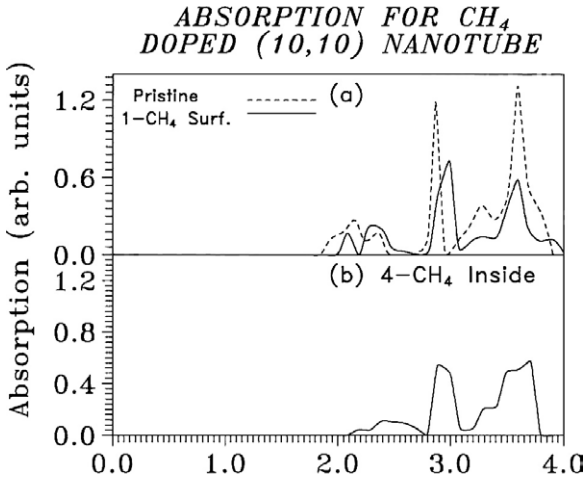

Figure 10. Absorption spectra in the energy range of 0–4.0 eV for the (10, 10) nanotube: (a) pristine and one CH_4 molecule on surface site, and (b) four CH_4 molecules inside the tube.

(3, 3) nanotube. The optical absorption along the tube axis for the pristine (3, 3) nanotube is shown in figure 8(a). One observes a strong peak having its low energy edge at 2.8 eV. This peak is quite close to the experimentally observed peak at 3.1 eV by Lie *et al* (2001) and Liang *et al* (2002) for a mixture of 4 Å nanotubes. The present value of 2.8 eV is also near to the calculated values by Machon *et al* (2002) and by Liu and Chan (2003) who have obtained peak at 2.8 eV. Spataru *et al* (2004) have also obtained a peak at 2.83 eV in the LDA and have shown that the consideration of the many-body effects including the excitonic contribution will raise the peak to 3.17 eV, which is closer to the experimental value of 3.1 eV. They have reported that a partial compensation takes place between the self-energy and the excitonic effects, and their combined effect on the optical absorption leads to a result which approaches towards LDA. A similar conclusion has also been drawn recently by Bruno *et al* (2005).

The transition between the states numbered as 24th and 25th at $k_z = 0$ are forbidden by symmetry considerations. It should be noted that appreciable optical absorption for the (3, 3) nanotubes, whether pristine or doped with the CH_4 molecule, is observed only for the wavevector range of $k_z = 0.38$–0.48. Also, the main peak at 2.8 eV arises from the transitions between the doubly degenerate occupied (23, 24)th and the unoccupied (25, 26)th states in the wavevector range of $k_z = 0.4$–0.48 as shown in figure 2(a). The other peaks involve the transitions between the filled (23, 24) states and the vacant (25–27) states. It may be cautioned that the present numbering of states is changed at different values of $k_z > 0.40$ and is totally different from the numbering of states at $k_z = 0$.

One CH_4. For the (3, 3) nanotube having one CH_4 per unit cell adsorbed on the surface, the peak structure (figure 8(a)) is quite similar to that of the undoped tube except the shifting of the edge of the strong absorption to 2.9 eV.

For the CH_4-doped (3, 3) tube too, as regards the participation of the states giving rise to absorption, the situation is exactly similar to that of the pristine tube (see figure 2(b)) except in the enhanced numbering of the participating states, which are increased by four because of the adsorption of a CH_4 molecule.

(5, 0) nanotube. The optical absorption for the pristine (5, 0) nanotube shown in figure 8(b) reveals two broad strong peaks centred at 0.8 and 2.5 eV. The present peaks are quite near to the experimental peaks observed at 1.2, 2.1 and 3.1 eV for a mixture of 4 Å carbon tubes by Lie *et al* (2001) and Liang *et al* (2002). Also, the present peaks are quite close to the calculated values of 1.2 and 2.3–2.4 eV by Machon *et al* (2002) and Liu and Chan (2003). Spataru *et al* (2004) have also obtained a peak at 1.13 eV in the LDA and have shown that the discrepancy between the LDA value and the experimental value can be explained if one also considers the many-body effects, including the excitonic contribution. The experimental peak at 1.2 eV is assigned to the (5, 0) tube. It may be mentioned that the optical absorption arises mainly from the wavevector range $k_z = 0$–0.08 and involves all the 37th to 45th states at different values of k_z. The transitions between the occupied (40, 41) and the unoccupied (42, 43) states are forbidden by symmetry considerations. The peak around 0.8 eV arises from the transition between the doubly degenerate occupied (38, 39) states and the doubly degenerate unoccupied (42, 43) states (see figure 3(a)). On the other hand, the peak at 2.5 eV originates from the transitions between the (40, 41) and the (44, 45) states. The weak absorption arising from the wavevector range of $k_z = 0.08$–0.24 appears in the high energy region above 3.0 eV.

One CH_4. For the (5, 0) nanotube doped with one CH_4 on the surface, the absorption presented in figure 8(b) reveals strong peaks at 1.0 and 2.4 eV. An extra quite weak peak appears at 0.5 eV. The participation of the states in the absorption at 1.0 eV are exactly similar to those seen earlier in the pristine (5, 0) tube except for the altered numbering of the participating states which are now the valence (42, 43) states and the conduction (46, 47) states (see figure 3(b)). Similar to the pristine (5, 0) tube, weak absorption above 3.0 eV is seen for the wavevector range of $k_z = 0.12$–0.24. For more than one CH_4 molecule adsorbed on the (5, 0) nanotube, the absorption is expected to have a similar nature.

(4, 2) nanotube. The optical absorption for the pristine (4, 2) nanotube as shown in figure 8(c) reveals a peak at 2.0 eV along with three very weak peaks at 2.7, 2.9 and 3.6 eV. The strong peak at 2.0 eV originates from the transitions between the occupied (107, 108, 111) states and the unoccupied (115, 116, 118) states, as has been shown in figure 4(a).

Our peaks are in good agreement with the measured peaks at 2.1 and 3.1 eV for a mixture of 4 Å carbon tubes by Lie *et al* (2001) and Liang *et al* (2002) and the calculated peaks at 1.9, 2.9–3.0 and 3.6 eV by Machon *et al* (2002) and Liu and Chan (2003). The case of the (4, 2) tube has not been discussed by Spataru *et al* (2004) because of the big size of the unit cell. Chang *et al* (2004) used an *ab initio* many body approach considering also the excitonic effects for the pristine (4, 2) tube and obtained extra peaks arising from the exciton states along with the usual peaks in the one-electron approximation.

For one CH_4 molecule residing on the surface of the (4, 2) tube, the optical absorption is shown in figure 8(c). Similar to the pristine (4, 2) nanotube, a very strong peak appears at 1.90 eV. which arises from the transitions between the occupied (111, 112, 115, 116) states and the unoccupied (117, 118, 121, 122) states (see figure 4(b)). Other weak peaks are also present.

(10, 0) nanotube. The optical absorption for the pristine (10, 0) nanotube as shown in figure 9(a) reveals four peaks at 0.9, 2.1, 2.6 and 3.0 eV. The present peaks at 0.9 and 2.1 eV for the (10, 0) tube having a diameter of 7.85 Å are quite near to the experimental peaks observed at 0.95, 1.12, 1.8 and 2.25 eV measured both in the absorption and emission by O'Connell *et al* (2002) in a mixture of single walled nanotubes possessing tube diameters in the range of 7–11 Å.

It may be mentioned that the peaks at 2.25 and 3.5 eV in the optical absorption have been reported by the present authors (Agrawal *et al* 2003) for the isolated armchair (6, 6) nanotube of diameter 8.19 Å. The peak at 2.25 eV is in excellent agreement with the experimental data of O'Connell *et al* (2002).

The optical absorption arises mainly from the wavevector range of $k_z = 0$–0.08 and involves all the 73rd to 89th states at different values of k_z. The peak around 0.9 eV arises from the transitions between the occupied doubly degenerate (79, 80) states and the unoccupied doubly degenerate (81, 82) states as has been shown in figure 5(a). On the other hand, the peak at 2.1 eV originates from the transitions between the occupied (77, 78) and the unoccupied (88, 89) states. The other high energy peak at 2.6 eV corresponds to the transitions between the filled (75, 76) states and the vacant (86, 87) states, whereas the peak at 3.0 eV is generated by the occupied (73, 74) and the unoccupied (83–85) states.

One CH_4. For one CH_4 molecule adsorbed on the surface lying at the mid-hexagonal site on the (10, 0) nanotube, the absorption presented in figure 9(a) reveals again four peaks, but all shifted. The peaks appear at 0.7, 2.2, 2.5 and 2.9 eV.

For the endohedral adsorption, the optical absorption is presented in figure 9(b). The overall peak structure is similar to the exohedral adsorption except changes in the relative intensities of the peaks. The actual locations of the peaks are 0.75, 2.2, 2.5 and 3.1 eV.

The participations of the states in the absorption at 0.9 eV are exactly similar to those seen earlier in the pristine (10, 0) tube except the numberings of the participating states, which are enhanced by 4. The participating states giving rise to the peak at 0.9 eV are the valence (83, 84) states and the conduction (85, 86) states (see figure 5(b)). Similar arguments are valid for the other peaks.

(10, 10) nanotube. For the pristine (10, 10) nanotube, the optical absorption along the tube axis is shown in figure 10(a). One observes broad weak absorption around 2.2 eV and appreciable absorption in the energy range of 2.8–4.0 eV, including two strong peaks at 2.9 and 3.6 eV. The present two peaks are quite close to two of the four experimental peaks observed at 0.7, 1.3, 1.9 and 2.6 eV in the mixture of SWNTs of 14 Å diameter by Hwang *et al* (2000).

Kazaoui *et al* (2000) have also observed peaks at 1.2, 1.8 and 2.4 eV in a mixture of isolated and bundles of tubes having diameters in the range of 12–16 Å. Variation in the peak positions with the tube diameter lying in the range of 9–14 Å in the bundles of tubes have been reported by Liu *et al* (2002). In the experiments, a peak at 0.7 eV has been reported which is not seen in our calculation for the pristine (10, 10) nanotube. This low energy peak may arise from the same diameter tubes of other chiralities present in the measured sample. The predicted peak structure near 3.6 eV has not been reported as yet to the knowledge of the authors.

The transition between the states numbered as 80th and 81st at $k_z = 0$ is forbidden by symmetry considerations. As noted for the armchair (3, 3) tube, here too appreciable optical absorption for the nanotubes whether pristine or doped with the CH_4 molecule is observed only for the wavevector range of $k_z = 0.38$–0.44. The weak peak at 2.2 eV arises from the transitions between the occupied doubly degenerate (78, 79) and the unoccupied (82, 83) states as shown in figure 6(a). The other peak at 2.9 eV arises from the combinations of the occupied (76, 77) states and the unoccupied (84, 85) states. The highest energy peak at 3.6 eV originates from the combinations of the valence (74–79) and the conduction (83–91) states.

One CH_4. For the (10, 10) nanotube having one CH_4 molecule per unit cell adsorbed on the surface of the tube, the peak structure (figure 10(a)) is quite similar to that of the pristine tube except changes in the relative intensities of the peaks. Two strong peaks occur at 3.0 and 3.6 eV, whereas two weak peaks appear at 2.1 and 2.3 eV. For one CH_4-doped (10, 10) nanotube too, as regards the participation of the states giving rise to absorption, the situation is exactly similar to that of the pristine tube except in the enhanced numberings of the participating states, which are increased by four (see figure 6(b)). For the endohedral adsorption of four CH_4 molecules per unit cell, the peak structure as shown in figure 10(b) is quite the same except changes in the relative intensities of most of the peaks. A broad weak absorption is seen in the energy range of 2.1–2.7 eV and strong broad absorption appears at 2.9 and 3.6 eV.

4. Conclusions

The most favoured sites for the CH_4 molecule adsorption lie inside the large diameter tubes. One observes chirality dependence in the binding of the CH_4 molecules on the different types of nanotubes. The BEs of the CH_4 molecule adsorption are similar on both the achiral armchair (n, n) and the zigzag $(n, 0)$ tubes. We do not find any adsorption on the chiral (4, 2) tube. We also observe chirality dependence in the binding of the CH_4 molecules on the different surface sites of the nanotubes. The adsorption of the CH_4 molecule is preferred on the mid-hexagonal sites of the achiral tubes except on the mid-bond sites of the (3, 3) tube. In the large diameter tubes, the binding of the endohedral CH_4 molecule is much stronger as compared to the binding on the surface.

The adsorption of the CH_4 molecule either on the interstitial sites of the bundles of the nanotubes or on the groove sites of the nanoropes of the 4 Å tubes is not favoured.

Quite small changes in the diameters of the nanotubes are induced by the adsorption of the CH_4 molecules. On the other hand, large buckling occurs in the (n, n) tubes, in contrast to either negligible or quite small buckling in the $(n, 0)$ tubes. The minimum separation between the C atom of the CH_4 molecule and the host carbon atoms is quite similar in all the achiral 4 Å tubes.

The maximum admissible exohedral adsorption of the CH_4 molecules on all the surface sites of all the tubes is quite small. On the other hand, the maximal admissible endohedral adsorption in the large diameter (10, 0) and (10, 10) tubes will be 2.5% and 10% approx., respectively.

The binding of the CH_4 molecules on all the tubes originates from the dispersion forces, i.e. from the vdW energy, and one should not ignore vdW interactions in estimating the BE for the weakly bound adsorbates. We also find that the LDA over-binds the CH_4 molecule and the GGA under-binds it, and for a reliable theoretical estimate one should take an average of the BEs determined in the LDA and GGA.

In view of the idealized nature of the present calculation and the uncertainty in the measurements, the currently calculated values for the binding energy and the adsorbate concentration are in reasonable agreement with the measured data available for the (10, 10) nanotubes.

The electronic structure of the pristine tube is changed by the adsorption of the CH_4 molecule on the surface of the tube because of the breaking of the symmetry of the host lattice except the chiral (4, 2) tube, which has practically no symmetry. It incurs splitting in the states in the whole energy range, especially in the large curvature 4 Å tubes. In the case of the armchair (n, n) tubes, the adsorption of the CH_4 molecule raises one valence state up to E_F and converts it into a mixed C(p)–H(s, p) state. The bandgap of the semiconducting achiral zigzag nanotube is reduced by the adsorption of the CH_4 molecule. On the other hand, the bandgap of a chiral semiconducting tube is enhanced by the adsorption of the CH_4 molecule.

The adsorption of one CH_4 molecule on all the tubes does not alter the peak structure in the optical absorption seen for the pristine tubes, except their changed energy locations and the relative intensities in the achiral tubes. Most of the calculated peaks in the optical absorption of the pristine large diameter (10, 0) and (10, 10) nanotubes have been observed in a number of experimental measurements.

Acknowledgments

The authors express thanks to the University Grants Commissions and Defence Research Development Organization, New Delhi, for financial assistance, and to Dr P S Yadav for providing us with the computation facilities.

References

Agrawal B K, Agrawal S and Srivastava R 2003 *J. Phys.: Condens. Matter* **15** 6931
Agrawal B K, Agrawal S, Srivastava R and Singh S 2004 *Phys. Rev.* B **70** 075403
Ajayan P M, Ebbesen T W, Ichihashi T, Ijima S, Tanigaki K and Hiura H 1993 *Nature* **362** 522
Akai Y and Saito S 2003 *Japan. J. Appl. Phys.* **42** 640
Becke A D 1988 *Phys. Rev.* A **38** 3098
Bruno M, Palummo M, Marini A, Sole R D, Olevano V, Kholod A N and Ossicini S 2005 *Phys. Rev.* B **72** 153310
Chang F, Bussi G, Ruini A and Molinari E 2004 *Phys. Rev. Lett.* **92** 196401
Collins P G, Bradley K, Ishigami M and Zettl A 2000 *Science* **287** 1801
Dag S, Gulseren O, Yildirim T and Ciraci S 2003 *Phys. Rev.* B **67** 165424
Durgun E, Dag S, Bagei V M K, Gulseren O, Yildirim T and Ciraci S 2003 *Phys. Rev.* B **67** 201401 and the references therein
For a review of earlier work see Dresslhaus M S, Williams K A and Eklund P C 1999 *MRS Bull.* **24** 45
Fuchs M and Scheffler M 1999 *Comput. Phys. Commun.* **119** 67
Goedecker S 1997 *SIAM J. Sci. Comput.* **18** 1605
Gonze X 1996 *Phys. Rev.* B **54** 4383
Halgren T A 1992 *J. Am. Chem. Soc.* **114** 7827
Hirscher M, Becher M, Haluska M, Quintel A, Skakalova V, Choi Y M, Dettlaff-Weglikowska U, Roth S, Stepanek I, Bernier P, Leonhardt A and Fink J 2002 *J. Alloys Compounds* **330** 654
Hwang H, Gommans H H, Ugawa A, Tashiro H, Haggenmueller R, Winey K I, Fischer J E, Tanner D B and Rinzler A G 2000 *Phys. Rev.* B **62** R13310
Hybertson M S and Needles M 1993 *Phys. Rev.* B **48** 4608

Kazaoui S, Minami N, Yamawaki H, Aoki K, Kataura H and Achiba Y 2000 *Phys. Rev.* B **62** 1643
Kleinhammes A, Mao S H, Yang X J, Tang X P, Shimoda H, Lu J P, Zhou O and Wu Y 2003 *Phys. Rev.* B **68** 075418
Kleinman L and Bylander D M 1982 *Phys. Rev. Lett.* **48** 1425
Kong J, Franklin N R, Zhou C W, Chapline M G, Peng S, Cho K J and Dai H J 2000 *Science* **287** 622
Liang W, Chen G, Li Z and Tang Z K 2002 *Appl. Phys. Lett.* **80** 3415
Lie Z M, Tang Z K, Liu H J, Wang N, Chan C T, Saito R, Okada S, Li G D, Chen J S, Nagasawa N and Tsuda S 2001 *Phys. Rev. Lett.* **87** 127401
Liu H J and Chan C T 2003 *Solid State Commun.* **125** 77
Liu X, Pichler T, Knupfer M, Golden M S, Fick J, Kataura H and Achiba Y 2002 *Phys. Rev.* B **66** 045411
Machon M, Reich W, Thomson C, Sanchez-Portal D and Ordejon P 2002 *Phys. Rev.* B **66** 155410
Mackie E B, Wolfson R A, Arnold L M, Lafdi K and Migone A D 1997 *Langmuir* **13** 7197
Muris M, Dufau N, Bienfait M, Dupont-Pavlovsky N, Grillet Y and Palmari J P 2000 *Langmuir* **16** 7019
O'Connell M J, Bachilo S M, Huffman C B, Moore V C, Strano M S, Haroz E H, Rialon K L, Boul P J, Noon W H, Kittrell C, Ma J, Hauge R H, Weisman R B and Smalley R E 2002 *Science* **297** 593
Payne M C 1992 *Rev. Mod. Phys.* **64** 1045
Perdew J P, Burke K and Ernzerhof M 1996 *Phys. Rev. Lett.* **77** 3865
Saito Y, Nishiyama T, Kato T, Kondo S, Tanaka T, Yotani J and Uemura S 2002 *Mol. Cryst. Liq. Cryst.* **387** 303
Schlapbach M and Zuttel M 2001 *Nature* **414** 353
Shi W and Johnson J K 2003 *Phys. Rev. Lett.* **81** 015504
Shim M, Kam N W S, Chen R J, Li Y M and Dai H J 2002 *Nano Lett.* **2** 285
Skoulidas A I, Ackerman D M, Johnson J K and Shool D S 2002 *Phys. Rev. Lett.* **89** 185901
Spataru C D, Beigi S I, Benedict L X and Louie S G 2004 *Phys. Rev. Lett.* **92** 77402
Stan G, Bojan M J, Curtarolo S, Gatica S M and Cole M W 2000 *Phys. Rev.* B **62** 2173
Sumanasekera G U, Adu C K W, Fang S and Eklund P C 2000 *Phys. Rev. Lett.* **85** 1096
Talapatra S and Migone A D 2000 *Phys. Rev.* B **65** 045416
Talapatra S, Zambano A J, Weber S E and Migone A D 2000 *Phys. Rev. Lett.* **85** 138
Tanaka H, EL-Merraouli M, Steele W A and Kaneko K 2002 *Chem. Phys. Lett.* **352** 334
Troullier N and Martins J L 1991 *Phys. Rev.* B **43** 1993
Tsang S C, Chen Y K, Harris P J F and Green M L H 1994 *Nature* **372** 159
Weber S E, Talapatra S and Migone A D 2000 *Phys. Rev.* B **61** 13150
Zhao J, Buldum A, Han J and Lu J P 2002 *Nanotechnology* **13** 195